Supporting information

Hierarchical bilayered hybrid nanostructural arrays of $NiCo_2O_4$ microurchins and nanowires as free-standing electrode with high loading for high-performance lithium-ion batteries

Yu Wang,[a,c] Pengcheng Liu,[b]* Kongjun Zhu,[a]* Jing Wang,[a] Jinsong Liu[a,c]

[a] State Key Laboratory of Mechanics and Control of Mechanical Structures, Nanjing University of Aeronautics and Astronautics, Nanjing 210016, China

[b] School of Mechanical and Electric Engineering, Guangzhou University, Guangzhou 510006

[c] China College of Materials Science and Engineering , Nanjing University of Aeronautics and Astronautics, Nanjing 210016, China

Corresponding Author: kjzhu@nuaa.edu.cn (K. Zhu); pch060710111@hotmail.com (P. Liu)

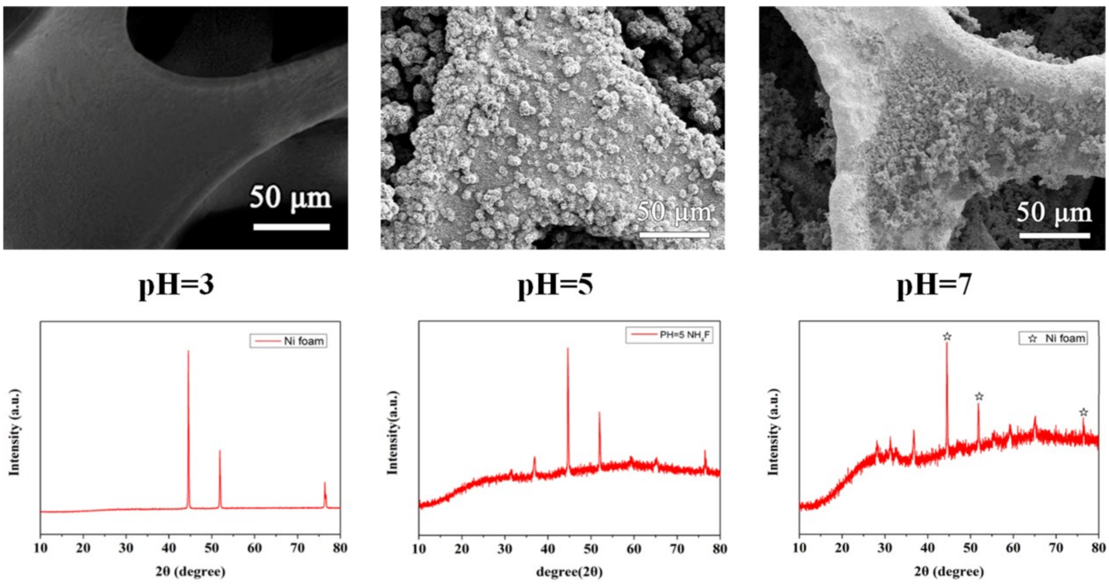

Figure S1. SEM images and the corresponding XRD images of these products prepared in pH=3, pH=5, pH=7 under hydrothermal condition, respectively.

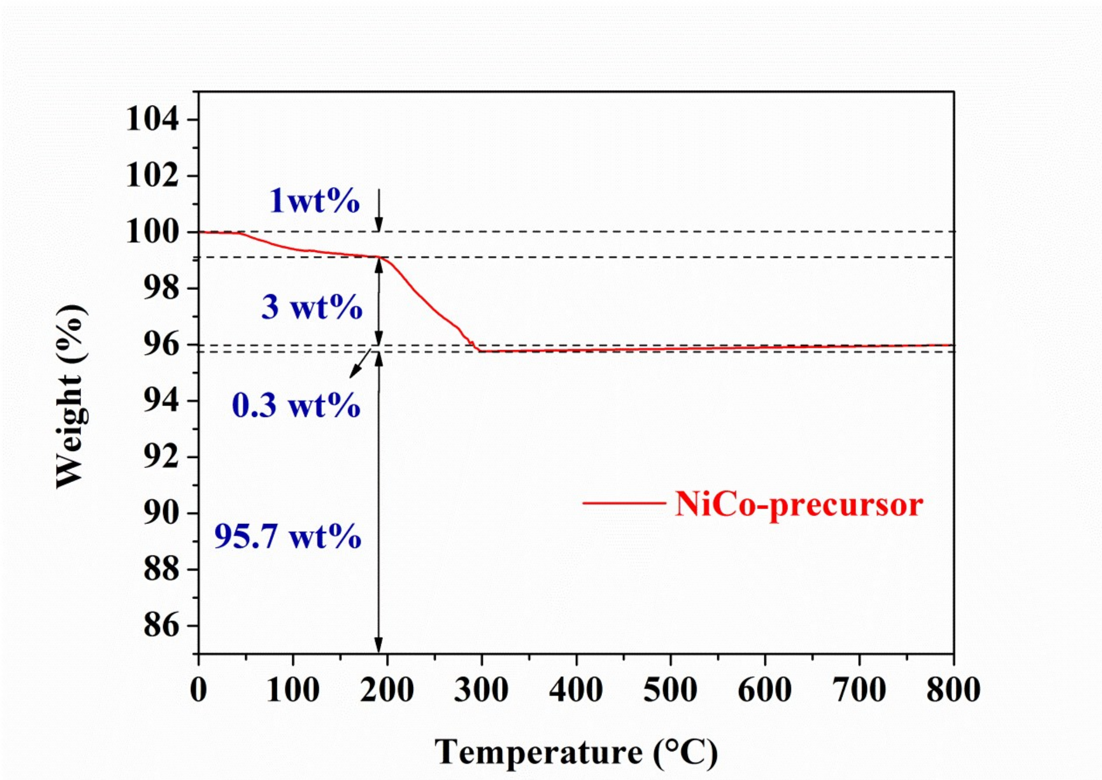

Figure S2 TG measurement of NiCo-precursor HNAs at a temperature range of 0-800 °C and the heating rate 10 °C /min

To further confirm the calcination temperature during annealing, we conduct the TG measurement of NiCo-precursor HNAs at a temperature range of 0-800 °C with a heating rate of 10 °C /min, and the TG data is shown in Figure R1. The XRD pattern of the Ni-Co precursors, which may be mixture of $Co_2(CO_3)(OH)_2 \cdot 0.11H_2O$ and $Ni_2(CO_3)(OH)_2 \cdot 4H_2O$, is shown in Figure R2. In Figure R1, the initial 1 % mass loss between 50 and 200 °C is due to the evaporation of moisture. The large mass loss of about 3 % between 200 and 300 °C can be observed, which is attributed to the release of CO_2 and hydrolysis during the transformation from $Co_2(CO_3)(OH)_2 \cdot 0.11H_2O$ and $Ni_2(CO_3)$ $(OH)_2 \cdot 4H_2O$ to $NiCo_2O_4$. The mass have a slight increase during the following temperature rise, which may be caused by the oxidation of metallic Ni. Thus, selecting 300 °C as the annealing temperature can not only ensure the complete transformation from $Co_2(CO_3)(OH)_2 \cdot 0.11H_2O$ and $Ni_2(CO_3)$ $(OH)_2 \cdot 4H_2O$ to $NiCo_2O_4$, but also avoid the excessive oxidation of nickel foam. In addition, our dense $NiCo_2O_4$ HNAs on NF can have an effect to prevent the oxidation of NF during annealing. So, the calcination temperature was finally set as 300 °C.

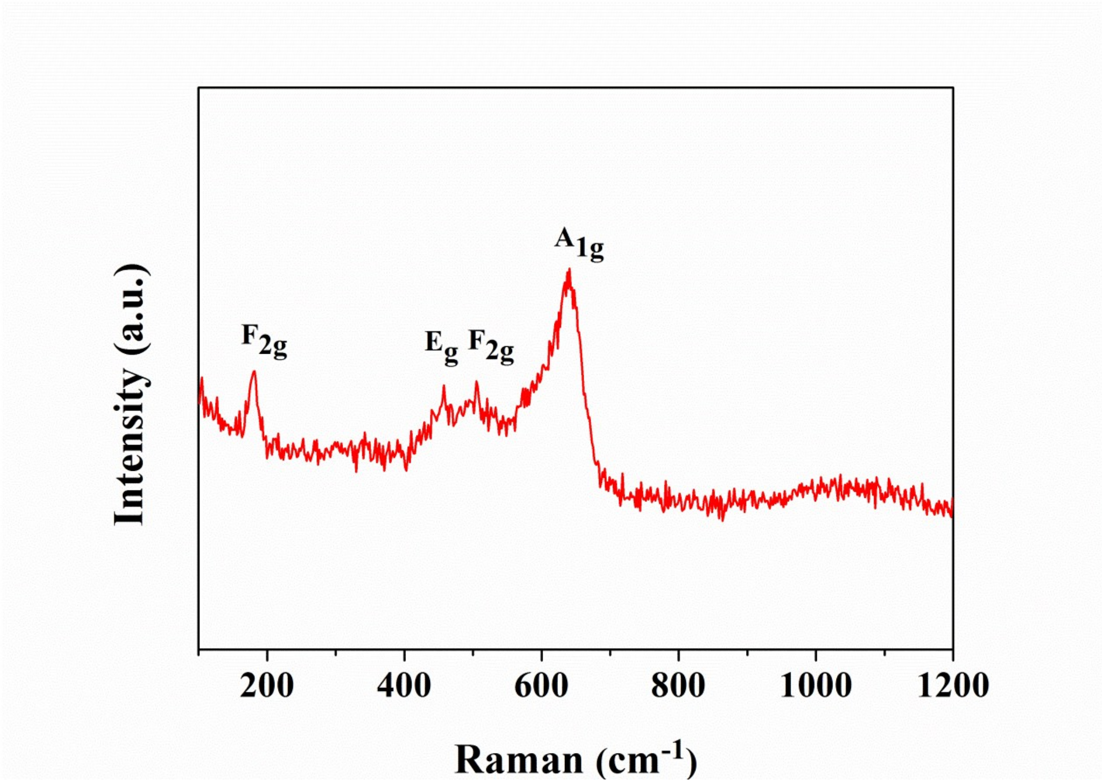

Figure S3 Raman spectra of $NiCo_2O_4$ HNAs.

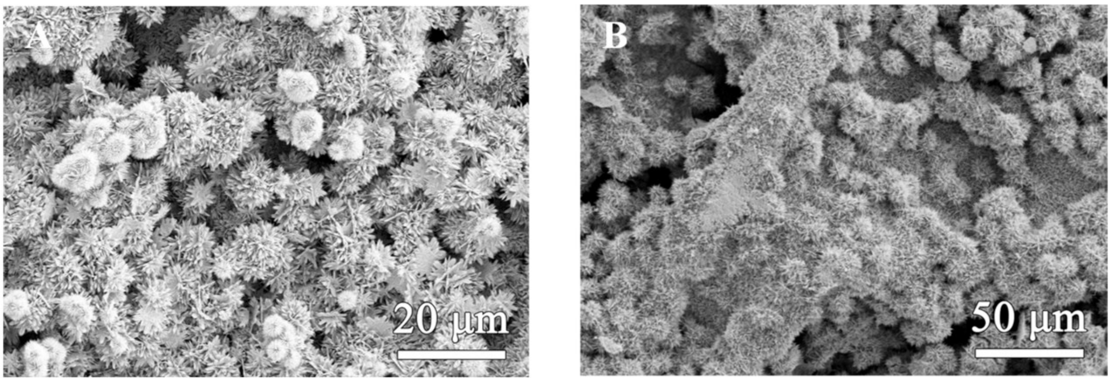

Figure S4 The SEM images of $NiCo_2O_4$ HNAs before and after ultrasonic treatment.

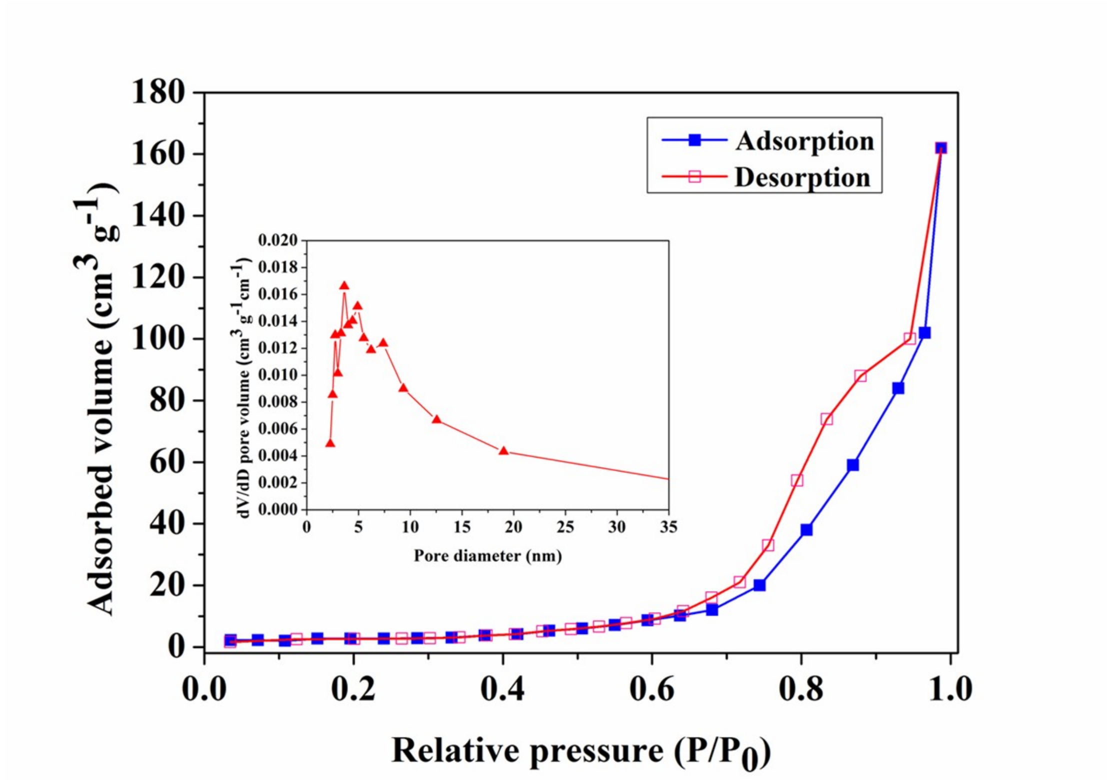

Figure S5 Nitrogen adsorption/desorption isotherms and pore-size distribution curves for $NiCo_2O_4$ HNAs.

Table S1. Electrochemical performance of different $NiCo_2O_4$ electrodes.

Type of materials	Capacity	Rate performance	Cycling stability	loading (mg/cm^2)	Reference
$NiCo_2O_4$ HNAs/NF	1094 mAh g^{-1} (at 500mA g^{-1})	875 mAh g^{-1} (at 1000 mA g^{-1})	90 % (After 100 cycles at 500 mA g^{-1})	7	This work
$NiCo_2O_4$ NWAs/ CT	1012 mAh g^{-1} (at 500mA g^{-1})	589 mAh g^{-1} (at 3000 mA g^{-1})	84 % (After 100 cycles at 500 mA g^{-1})	1.2	1
$NiCo_2O_4$@ $NiCo_2O_4$ Nanocactus/NF	925 mAh g^{-1} (at 120 mA g^{-1})	407 mAh g^{-1} (at 960 mA g^{-1})	90% (After 100 cycles at 120 mA g^{-1})	3.0	2
$NiCo_2O_4$ complex hollow spheres	1401 mAh g^{-1} (at 150 mA g^{-1})	533 mAh g^{-1} (at 2000 mA g^{-1})	78% (After 100 cycles at 200 mA g^{-1})	-	3

$NiCo_2O_4$/C nanocomposites	1154 mAh g^{-1} (at 40 mA g^{-1})		78.3% (After 50 cycles at 40 mA g^{-1})	-	4
flower-like $NiCo_2O_4$	~1280 mAh g^{-1} (at 150 mA g^{-1})	420 mAh g^{-1} (at 2000 mA g^{-1})	~55% (After 60 cycles at 500 mA g^{-1})	-	5
$NiCo_2O_4$ microspheres	~1680 mAh g^{-1} (at 100 mA g^{-1})	393 mAh g^{-1} (at 1600 mA g^{-1})	~53% (After 70 cycles at 800 mA g^{-1})	-	6
$NiCo_2O_4$–RGO composite	1351 mAh g^{-1} (at 100 mA g^{-1})	396 mAh g^{-1} (at 800 mA g^{-1}	80.1% (After 70 cycles)	-	7

References

1 L. F. Shen, Q. Che, H. S. Li and X. G. Zhang, Adv. Funct. Mater. 2014, 24, 2630–2637.

2 J. B.Cheng, Y. Luo, Y. Lu, K.Q. H. L. Yan. et al. Sci. Rep. 5, 12099; doi: 10.1038/srep12099 (2015).

3 L. F. Shen, L. Yu, X.Y. Yu, X. G. Zhang, and X. W. (David) Lou. Angew. Chem. Int. Ed. 2015, 54, 1868 –1872.

4 Y. N. NuLi, P. Zhang, Z. P. Guo, H. K. Liu, J. Yang, Electrochem.Solid-State Lett. 2008, 11, A64.

5 L. L. Li, Y. Cheah, Y.W. Ko, P. Teh, G. Wee, C. L. Wong, S. J.Peng, M. Srinivasan, J. Mater. Chem. A 2013, 1, 10935.

6 J. F. Li, S. L. Xiong, Y. R. Liu, Z. C. Ju, Y. T. Qian, ACS Appl.Mater. Interfaces 2013, 5, 981.

7 Y. J. Chen, M. Zhuo, J.W. Deng, Z. Xu, Q. H. Li, T. H. Wang, J.Mater. Chem. A 2014, 2, 4449.